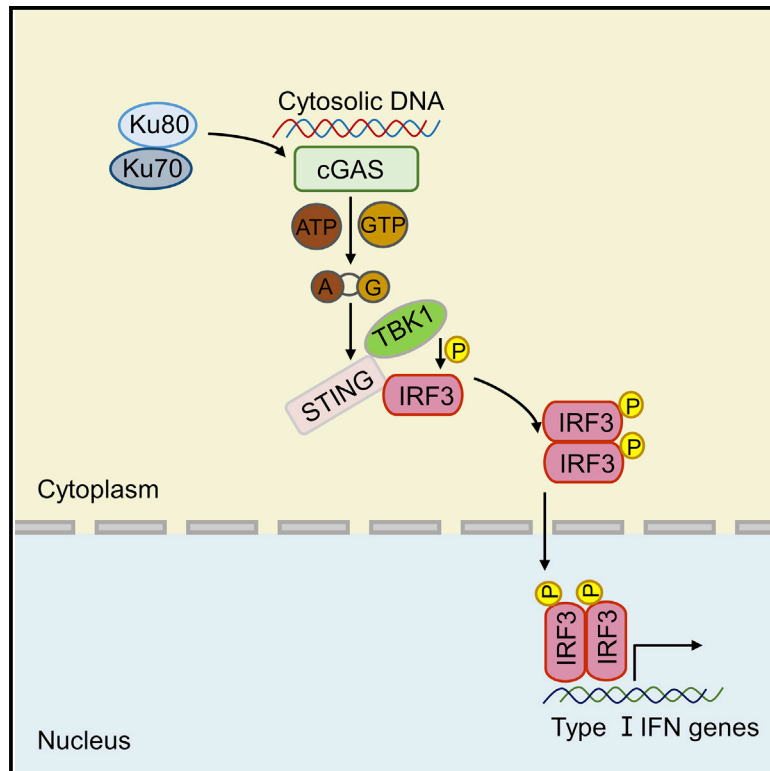


Ku proteins promote DNA binding and condensation of cyclic GMP-AMP synthase

Graphical abstract



Authors

Xinyue Tao, Jiali Song, Ying Song, ...,
Dechong Zhang, Dahua Chen,
Qinmiao Sun

Correspondence

chendh@ynu.edu.cn (D.C.),
qinmiaosun@ioz.ac.cn (Q.S.)

In brief

Tao et al. show that Ku proteins act as co-sensors of cGAS. Ku proteins augment cGAS catalytic activity by increasing the DNA binding affinity of cGAS and promoting cGAS condensation, thus ensuring an efficient innate immune response to DNA virus infection.

Highlights

- The Ku proteins, Ku80 and Ku70, interact with cGAS and augment cGAS-mediated signaling
- Ku proteins increase the DNA binding affinity of cGAS and promote cGAS condensation
- The cGAS-Ku protein interaction increases the catalytic activity of cGAS
- Ku proteins function as co-sensors of cGAS to regulate cGAS-STING signaling



Article

Ku proteins promote DNA binding and condensation of cyclic GMP-AMP synthase

Xinyue Tao,^{1,3,4,5} Jiali Song,^{2,5} Ying Song,² Yao Zhang,² Jing Yang,^{1,3} Pengfei Zhang,^{1,3} Dechong Zhang,² Dahua Chen,^{2,*} and Qinmiao Sun^{1,3,6,*}

¹State Key Laboratory of Membrane Biology, Institute of Zoology, Chinese Academy of Sciences, Jia #3 Datun Road, Chaoyang District, Beijing 100101, China

²Institute of Biomedical Research, Yunnan University, Kunming 650500, China

³Institute of Stem Cells and Regeneration, Chinese Academy of Sciences, Beijing 100101, China

⁴School of Life Sciences, University of Chinese Academy of Sciences, Beijing 100049, China

⁵These authors contributed equally

⁶Lead contact

*Correspondence: chendh@ynu.edu.cn (D.C.), qinmiaosun@ioz.ac.cn (Q.S.)

<https://doi.org/10.1016/j.celrep.2022.111310>

SUMMARY

Cyclic GMP-AMP synthase (cGAS) is a cytosolic DNA sensor that plays a critical role in regulating antiviral signaling. cGAS binds to DNA and catalyzes the synthesis of cyclic GMP-AMP (cGAMP), which is essential for downstream signal transduction. The antiviral response is a rapid biological process; however, cGAS itself has relatively low DNA binding affinity, implying that formation of the cGAS-DNA complex requires an additional factor(s) that promotes cGAS-DNA binding, allowing efficient antiviral signal transduction. Here, we report that the Ku proteins (Ku80 and Ku70) directly interact with cGAS and positively regulate cGAS-mediated antiviral signaling. Mechanistically, we find that the interaction of the Ku proteins with cGAS significantly increases the DNA-binding affinity of cGAS and promotes cGAS condensation in the cytosol, thereby enhancing cGAS catalytic activity. Our results show that the Ku proteins are critical partners of cGAS in sensing DNA virus infection and ensuring efficient innate immune signal transduction.

INTRODUCTION

The innate immune response against virus infection is initiated by the detection of an invading virus by pattern recognition receptors (Akira et al., 2006; Brubaker et al., 2015; Medzhitov, 2007). To recognize DNA viruses, in addition to the well-known endosomal Toll-like receptor 9 (TLR9) (Lund et al., 2003), a variety of cytosolic pattern recognition receptors have been identified, such as DNA-dependent activator of interferon-regulatory factors (DAI) (Takaoka et al., 2007), absent in melanoma 2 (AIM2) (Gray et al., 2016), interferon γ inducible protein 16 (IFI16) (Unterholzner et al., 2010), DDX41 (Zhang et al., 2011b), DNA-dependent protein kinase (DNA-PK) (Ferguson et al., 2012), meiotic recombination 11 homolog A (MRE11) (Kondo et al., 2013), stimulator of IFN genes (STING) (Burdette et al., 2011), SRY-box transcription factor 2 (SOX2) (Xia et al., 2015), polyglutamine binding protein 1 (PQBP1) (Yoh et al., 2015), and cyclic GMP-AMP synthase (cGAS) (Sun et al., 2013). Among these DNA sensors, only cGAS was identified as the universal cytosolic double-stranded DNA sensor that is independent of specificity of DNA sequence and/or cell type. cGAS can recognize not only foreign DNA from invading microbes, including bacteria, DNA viruses, and retroviruses, but also cytosol self-DNA leaked from the nuclear or mitochondrial compartment. Thus, cGAS plays a critical role in the innate immune response against both DNA virus infection and

autoimmunity (Collins et al., 2015; Gao et al., 2015; Li et al., 2013b; Schoggins et al., 2014; West et al., 2015). Upon binding to DNA, cGAS catalyzes the synthesis of cyclic GMP-AMP (cGAMP) from ATP and GTP (Gao et al., 2013a). cGAMP then binds to the endoplasmic reticulum membrane protein STING and activates the transcription factors IRF3 and NF- κ B through the TBK1/IKKi kinases and the IKK complex, respectively, thereby inducing the production of type I interferons (IFNs) and proinflammatory cytokines (Gao et al., 2013b; Wu et al., 2013).

Although cGAS has been identified as a major DNA sensor, its binding affinity for DNA is relatively low (dissociation constant in the range of 20 μ M to 80 nM) (Jonsson et al., 2017; Kranzusch et al., 2013; Li et al., 2013a; Zhang et al., 2014). How its low DNA binding affinity can efficiently mediate the complicated responses to a broad range of DNA ligands remains unclear. The low DNA binding affinity of cGAS suggests that co-sensors may function together with cGAS to mediate antiviral signaling. Indeed, ZCCHC3 (Lian et al., 2018) and PCBP1 (Liao et al., 2021) were shown to act as co-sensors to increase the DNA binding ability of cGAS. cGAS has been reported to detect a wide range of DNAs, including low amounts of pathogen DNA from bacteria and DNA viruses, as well as self-DNA in the cytosol (Collins et al., 2015; Gao et al., 2015; Li et al., 2013b; Schoggins et al., 2014; West et al., 2015). Therefore, we speculate that additional co-sensors are required to increase the DNA



binding affinity of cGAS to efficiently mediate antiviral signal transduction.

DNA-PK is a heterotrimeric protein complex composed of Ku70, Ku80, and a catalytic subunit (DNA-PKcs), which are encoded by *XRCC6*, *XRCC5*, and *PRKDC*, respectively. In addition to its nuclear localization, DNA-PK is partially localized in the cytoplasm (Ferguson et al., 2012; Huston et al., 2008). Several studies have shown that the DNA-PK complex functions as a DNA sensor to participate in the innate immune response to DNA virus infection (Burleigh et al., 2020; Ferguson et al., 2012; Wang et al., 2017; Zhang et al., 2011a). In the DNA-PK complex, Ku70 and Ku80 form a heterodimer (Ku proteins) that is important for the stability of each (Gu et al., 1997; Nussenzweig et al., 1996). The Ku proteins can directly bind to DNA and have strong binding affinities (Blair et al., 1993; Walker et al., 2001). The DNA-PKcs can also bind directly to DNA (Hammarsten and Chu, 1998), but its DNA binding affinity is remarkably decreased in the absence of the Ku proteins (Singleton et al., 1999; Yaneva et al., 1997). cGAS and the Ku proteins can both bind to DNA and are involved in modulating the innate immune response to DNA virus; however, whether the Ku proteins and cGAS coordinately regulate the innate immune response to DNA virus remains unclear.

In this study, we identified the Ku proteins as cGAS-interacting proteins, and the functional analysis suggested that Ku proteins play important roles in regulating the cGAS-mediated innate immune response. We also demonstrated that Ku proteins significantly enhance the DNA binding affinity of cGAS, and subsequently enhance cGAS condensation, thus augmenting cGAS catalytic activity. These findings support the idea that Ku proteins function as co-sensors to regulate the cGAS-mediated innate immune response to DNA virus infection.

RESULTS

Ku70 and Ku80 are cGAS-interacting factors

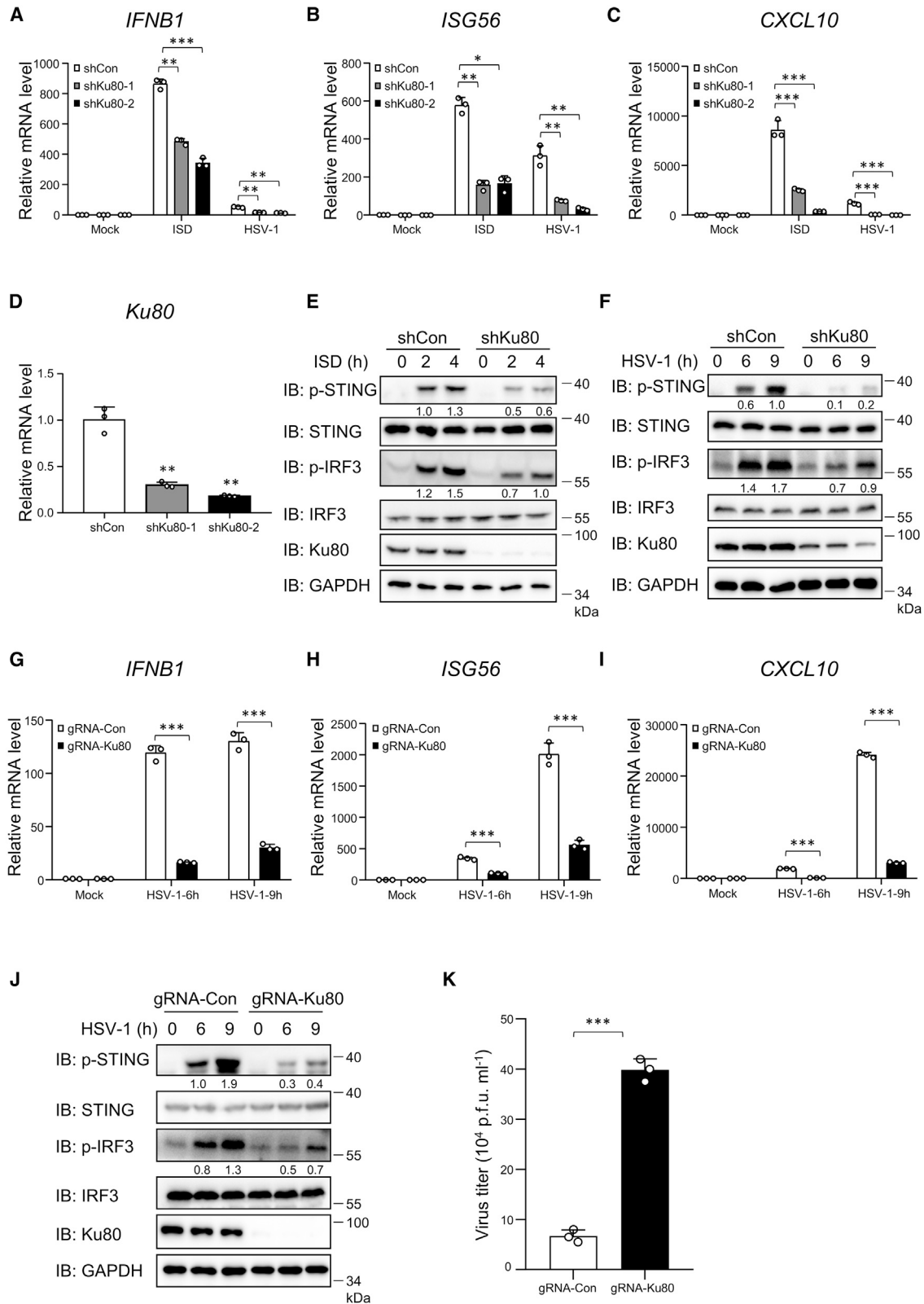
To better understand the molecular mechanisms underlying cGAS-mediated antiviral signal transduction, we identified cGAS-interacting proteins by co-immunoprecipitation (coIP) followed by mass spectrometry assays in HEK293A cells. We used S-protein-FLAG-streptavidin binding peptide (SFB)-tagged cGAS as bait (with an empty vector as the control) and identified a number of proteins that could potentially interact with cGAS.

Among these proteins, Ku80, Ku70, and DNA-PKcs were of particular interest because they are key components of the DNA-PK complex, which has been shown to mediate the innate immune response to virus infection (Burleigh et al., 2020; Ferguson et al., 2012; Zhang et al., 2011a). To validate the data obtained from the mass spectrometry analysis, we transfected HEK293A cells with FLAG-tagged cGAS and performed additional coIP assays using anti-FLAG M2 agarose beads. As shown in Figure 1A, FLAG-cGAS pulled down endogenous Ku80, Ku70, and DNA-PKcs. Next, we investigated how these key components of the DNA-PK complex interacted with cGAS. Because cGAS pulled down Ku80 and Ku70, and because the Ku proteins and DNA-PKcs form the DNA-PK complex, we next examined whether cGAS associated with the Ku proteins through DNA-PKcs. For this, we generated DNA-PKcs-knockout HEK293T cells, and then transfected them with FLAG-tagged cGAS or an empty vector. The coIP results indicated that DNA-PKcs deficiency had no effect on the association of cGAS with the Ku proteins, implying that the Ku proteins associated with cGAS in a DNA-PKcs-independent manner (Figure 1B). To determine whether cGAS directly interacted with Ku70 or Ku80, we performed *in vitro* pull-down experiments using purified recombinant His-tagged green fluorescent protein (His-GFP), His-cGAS-GFP, His-Ku80, or His-Ku70 from *Escherichia coli*. Using anti-GFP beads, we found that Ku80 and Ku70 were both directly pulled down by cGAS-GFP but not by GFP (Figures 1C and 1D). Together, these results show that Ku80 and Ku70 directly interact with cGAS.

Next, we conducted endogenous coIP in THP-1 cells using anti-cGAS antibody to determine whether cGAS associated with the Ku proteins under both normal physiological and viral infection conditions. The results showed that Ku80 and Ku70 were in the cGAS immunoprecipitants with or without the infection of herpes simplex virus type 1 (HSV-1), a DNA virus (Figure 1E). Interestingly, we found that HSV-1 infection enhanced the interaction of cGAS with Ku proteins, and the abundance of cGAS was increased upon HSV-1 infection. To determine whether this enhanced interaction of cGAS with Ku proteins was because of increased cGAS abundance or HSV-1 infection, we repeated the coIP using STING-knockout THP-1 cells in which cGAS was not induced by HSV-1 infection. The results showed that HSV-1 infection still increased the association of cGAS with Ku proteins (Figure 1F), indicating that HSV-1 infection

Figure 1. Ku80 and Ku70 are cGAS-interacting proteins

- (A) HEK293A cells were transfected with FLAG-cGAS or empty vector and lysed at 24 h after transfection for coIP with anti-FLAG M2 agarose beads and then analyzed by immunoblotting.
- (B) Similar to (A), except that wild-type (WT) and DNA-PKcs knockout HEK293T cells were transfected.
- (C and D) Purified His-tagged cGAS-GFP protein or His-tagged GFP from *E. coli* was incubated with anti-GFP agarose beads for 2 h, then His-tagged Ku80 (C) or His-tagged Ku70 (D) was added to the GFP-bound complexes and incubated for another 4 h. Immunoprecipitated complexes were then pulled down with anti-GFP agarose beads and analyzed by immunoblotting.
- (E) THP-1 cells were mock infected or infected by HSV-1 (3 MOI) for 12 h. Then, the cell lysates were immunoprecipitated with rabbit anti-cGAS antibody or control IgG and analyzed by immunoblotting.
- (F) Cell infection and coIP were performed as in (E), except that STING knockout THP-1 cells were used.
- (G) Schematic diagram of Ku80 domains (top). HEK293T cells were co-transfected with FLAG-cGAS and HA-Ku80 or its deletion variants. coIP assays were performed with HA beads and analyzed by immunoblotting (bottom).
- (H) Schematic diagram of cGAS domains (top). HEK293T cells were co-transfected with Myc-Ku80 and FLAG-cGAS or its truncation variants. coIP assays were performed with anti-FLAG M2 agarose beads and analyzed by immunoblotting (bottom).
- HA, hemagglutinin; IB, immunoblot; IP, immunoprecipitation; WCL, whole-cell lysate. See also Figure S1.



(legend on next page)

augmented the association of cGAS with Ku proteins. Consistent results were obtained from immunostaining assays (Figure S1A). These data suggest that Ku proteins were associated with cGAS.

We next performed domain mapping to determine which domains of cGAS and the Ku proteins were required for their interaction. Ku proteins contain three domains: an N-terminal von Willebrand A domain (vWA), a central Ku core domain (Core), and a C-terminal domain (CTD). The Ku80 CTD contains a DNA-PKcs binding domain, and the Ku70 CTD contains a distal SAF-A/B, Acinus and PIAS (SAP) domain (Fell and Schild-Poulter, 2015; Walker et al., 2001). To identify the Ku80 domain that interacts with cGAS, we generated three deletion variants of Ku80 in which the vWA, Core, or CTD domain was deleted. The coIP results showed that the Ku80 Core domain, but not the vWA or CTD domain, was required for the Ku80-cGAS interaction (Figure 1G). cGAS contains a less-conserved N-terminal disordered region and a highly conserved C-terminal catalytic domain that contains nucleotidyltransferase (NTase) and male abnormal 21 (Mab21) domains (Civril et al., 2013; Sun et al., 2013). To identify the cGAS domain that interacts with Ku80, we generated two truncated variants of cGAS, FLAG-cGAS-N (residues 1–160) and FLAG-cGAS-C (residues 161–522). The coIP results showed that the cGAS C-terminal catalytic domain, but not the N-terminal domain, was critical for the cGAS-Ku80 interaction (Figure 1H). Similarly, the coIP results showed that the Ku70 Core domain and the cGAS CTD were important for the Ku70-cGAS interaction (Figures S1B and S1C). The Ku70 CTD was also required for the Ku70-cGAS interaction (Figure S1B). Together, these results suggest that cGAS interacts with Ku proteins in a domain-dependent manner.

Ku proteins are important for the innate immune response to DNA virus infection

Having shown that Ku proteins directly interacted with cGAS in a DNA-PKcs-independent manner, we next investigated the specific roles of the Ku proteins in cGAS-mediated antiviral signaling. First, we used the lentivirus-mediated short hairpin RNA (shRNA) knockdown system to knock down Ku80 in THP-1 cells. The quantitative PCR (qPCR) analysis showed that Ku80 knockdown significantly reduced the mRNA levels of *IFNB1*, *ISG56*, and *CXCL10* induced by HSV-1 infection or by transfection with 45-bp IFN stimulatory DNA (ISD) (Figures 2A–2D). Western blotting showed that Ku80 knockdown reduced the levels of phosphorylated STING and IRF3 induced by ISD transfection or HSV-1 infection (Figures 2E and 2F). Next, we used the lentiCRISPR system to generate stable THP-1 cells tar-

geting Ku80 at the population level by selection with puromycin. The qPCR assays showed that Ku80 deficiency markedly reduced the mRNA levels of *IFNB1*, *ISG56*, and *CXCL10* induced by HSV-1 infection (Figures 2G–2I) or ISD transfection (Figures S2A–S2C). Consistently, the western blotting results showed that Ku80 deficiency reduced the levels of phosphorylated STING and IRF3 induced by HSV-1 infection (Figure 2J) or ISD transfection (Figure S2D). Next, to examine whether Ku80 has a conserved function in the innate immune response to DNA virus in mouse cells, we knocked down Ku80 in SV40-immortalized mouse embryonic fibroblasts (MEFs) and obtained consistent qPCR results upon HSV-1 infection (Figures S2E–S2H). Given that Ku80 modulated the production of IFNs induced by DNA virus infection, we investigated whether Ku80 regulated DNA virus replication. Wild-type and Ku80-deficient THP-1 cells were infected with HSV-1-GFP. As shown in Figure 2K, virus replication was significantly enhanced in the Ku80-deficient cells compared with that in the wild-type control cells. In addition, we sought to investigate whether Ku80 contributed to the innate immune response to RNA viruses. As shown in Figures S2I–S2L, Ku80 deficiency did not decrease the mRNA levels of *IFNB1*, *ISG56*, and *CXCL10* or the levels of phosphorylated IRF3 induced by the infection of Sendai virus, an RNA virus. Together, these findings suggest that Ku80 specifically plays a positive role in regulating anti-DNA viral signaling.

Previous studies showed that Ku70 and Ku80 worked together to regulate the DNA double-strand break repair pathway (Hammel et al., 2010; Jackson and Jeggo, 1995). To determine whether the function of Ku70 was similar to that of Ku80 in regulating the innate immune response against DNA virus infection, we used Ku70-knockdown or Ku70-deficient THP-1 cells. The qPCR results clearly showed that Ku70 knockdown or Ku70 deficiency significantly reduced the mRNA levels of *IFNB1*, *ISG56*, and *CXCL10* stimulated by ISD transfection or HSV-1 infection (Figures S3A–S3D and S4A–S4F). Western blotting also showed that Ku70 knockdown or Ku70 deficiency decreased the levels of phosphorylated STING and IRF3 induced by ISD transfection or HSV-1 infection (Figures S3E, S3F, S4G, and S4H). Together, these data provide evidence that Ku80 and Ku70 both play positive roles in modulating the innate immune response to DNA virus infection.

Ku proteins positively regulate cGAS-STING signaling by targeting cGAS

Given that cGAS, Ku80, and Ku70 were all required for the antiviral innate immune responses against DNA virus infection, and

Figure 2. Ku80 is important for the innate immune response to DNA virus infection

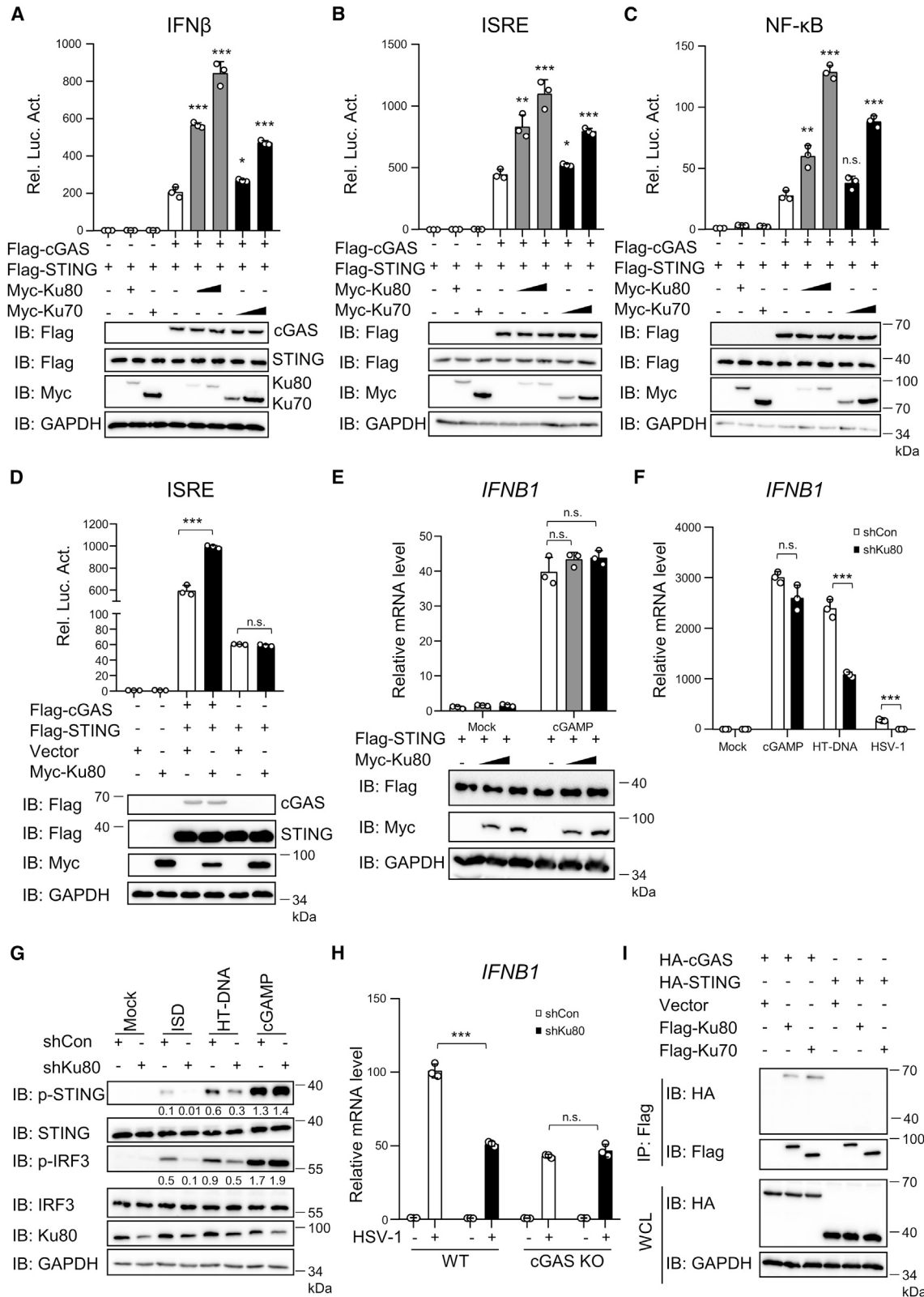
(A–D) THP-1 cells were infected with shRNA lentivirus targeting two different regions of Ku80 (shKu80-1, shKu80-2) or its control empty vector (shCon), followed by transfection with ISD (2 μg/mL) for 6 h or infection with HSV-1 (10 MOI) for 9 h. The cells were harvested for qPCR to measure mRNA levels of *IFNB1* (A), *ISG56* (B), *CXCL10* (C), and *Ku80* (D).

(E and F) THP-1 cells stably expressing shRNA targeting Ku80 or control cells were transfected with ISD (E) or infected with HSV-1 (F) for the indicated times and then analyzed by immunoblotting.

(G–J) THP-1 cells were transduced with single guide RNA (sgRNA) targeting Ku80 or control empty vector and then infected with HSV-1 (10 MOI) for 6 and 9 h and analyzed by qPCR to measure mRNA levels of *IFNB1* (G), *ISG56* (H), and *CXCL10* (I) or immunoblotted with the indicated antibodies (J).

(K) THP-1 cells were transduced with sgRNA targeting Ku80 or control empty vector and then infected with HSV-1-GFP (5 MOI) for 24 h. The culture supernatants were harvested to measure the virus titer by a plaque assay.

Data shown in (A–D, G–I, K) are from one representative experiment of at least three independent experiments (mean ± SD, n = 3 technical replicates in [A–D] and [G–I] and biological replicates in K). *p < 0.05, **p < 0.01, ***p < 0.001, two-tailed Student's t test. See also Figures S2, S3, and S4.



(legend on next page)

that the Ku proteins directly interacted with cGAS, we next investigated the functional relationship between cGAS and the Ku proteins. First, we examined the effects of Ku80 and Ku70 on the activity of cGAS by reporter assays. HEK293T cells stably expressing FLAG-STING were co-transfected with cGAS and a luciferase reporter driven by the IFN β promoter (IFN β -Luc) together with Ku80, Ku70, or an empty vector. Reporter assays showed that Ku80 and Ku70 alone did not activate the IFN β promoter; however, each of them significantly enhanced the activation of the IFN β promoter induced by cGAS overexpression in a dose-dependent manner (Figure 3A). Similar results were obtained when the IFN-stimulated response element (ISRE) and NF- κ B luciferase reporter were tested (Figures 3B and 3C). Notably, we found that Ku80 overexpression increased the activity of these promoters induced by cGAS to a much higher level than Ku70 overexpression did. Next, we examined whether Ku80 and Ku70 affected the activity of STING by reporter assays using the ISRE luciferase reporter and found that overexpression of Ku80 or Ku70 had no effect on the activity of the ISRE reporter induced by STING overexpression, whereas Ku80 or Ku70 overexpression increased the activity of the ISRE reporter induced by co-expression of cGAS and STING (Figures 3D and S5A). To further determine whether the Ku proteins specifically targeted cGAS but not STING, we examined whether the Ku proteins affected the activation of STING induced by cGAMP, which is synthesized by cGAS and binds to and activates STING. The qPCR analysis showed that overexpression of Ku80 or Ku70 did not affect the mRNA levels of *IFNB1* induced by cGAMP treatment in HEK293T cells stably expressing FLAG-STING (Figures 3E and S5B). Next, we knocked down Ku80 in THP-1 cells and found that Ku80 knockdown resulted in significantly reduced levels of *IFNB1* mRNA induced by herring testis DNA (HT-DNA) stimulation or HSV-1 infection, but not by cGAMP treatment (Figure 3F). Consistently, the western blotting results showed that Ku80 knockdown did not affect the levels of phosphorylated STING or IRF3 upon cGAMP treatment, whereas Ku80 knockdown had reduced effects on these factors upon ISD and HT-DNA stimulation (Figure 3G). We also knocked down Ku80 in cGAS-knockout THP-1 cells, then stimulated with HSV-1 infection, and found that, unlike in wild-type cells, knockdown of Ku80 in the cGAS-knockout cells did not reduce the mRNA levels of *IFNB1* induced by HSV-1 infection (Figures 3H and S5C). In addition, the colP results showed that

Ku80 and Ku70 specifically pulled down cGAS but not STING under the same colP conditions (Figure 3I). Together, these results suggest that Ku proteins act upstream of cGAMP, and target cGAS to modulate cGAS-cGAMP-STING signaling.

Ku proteins augment the enzymatic activity of cGAS by promoting its DNA binding

We next investigated the possibility that Ku proteins positively regulate cGAS signaling by promoting its catalytic activity, leading to increased production of cGAMP. First, we examined whether Ku80 or Ku70 knockdown affected cGAS activity induced by HT-DNA stimulation or HSV-1 infection in THP-1 cells and found that the production of cGAMP in Ku80- or Ku70-knockdown cells was significantly lower than it was in control cells (Figures 4A, 4B, and S5D). To exclude the influences of STING and its downstream signaling on the cGAS activity, we employed STING-knockout THP-1 cells, and found that even in the absence of STING, knockdown of Ku80 or Ku70 still reduced cGAMP production induced by HSV-1 infection (Figure S5D). Next, we used purified recombinant cGAS, Ku80, and Ku70 from *E. coli* and performed *in vitro* cGAMP synthesis assays by incubating cGAS with ATP, GTP, and HT-DNA in the presence or absence of Ku80 or Ku70. The results indicated that Ku80 significantly enhanced the production of cGAMP by cGAS upon HT-DNA stimulation, whereas, compared with Ku80, a high concentration of Ku70 was needed to increase cGAS activity (Figure 4C). Together, these results demonstrate that Ku80 and Ku70 both significantly promote cGAS signaling by regulating catalytic activity, especially Ku80.

Next, we investigated the molecular mechanism underlying how Ku proteins enhanced cGAS activity. Because Ku proteins and cGAS can bind to DNA, we hypothesized that Ku proteins likely affected the binding affinity of cGAS to DNA. To test this idea, we knocked down Ku80 or Ku70 in THP-1 cells and then transfected the cells with biotin-labeled ISD and performed pull-down experiments using streptavidin-Sepharose beads. As shown in Figure 4D, less cGAS was pulled down in the Ku80- or Ku70-knockdown cells than was pulled down in the control cells. Notably, knockdown of Ku70 or Ku80 resulted in destabilization of the other, which is consistent with previous results (Ferguson et al., 2012; Gu et al., 1997; Nussenzweig et al., 1996). Similar results were obtained when Ku80 was knocked down in MEFs (Figure S6A). Consistently, depletion of Ku80

Figure 3. Ku proteins target cGAS to positively regulate antiviral signaling

(A–C) HEK293T cells stably expressing FLAG-STING were co-transfected with the indicated expression plasmids and IFN β -Luc (A), ISRE-Luc (B), or NF- κ B-Luc (C) reporter. Cell lysates were analyzed by luciferase (top) and immunoblotting (bottom) assays.
(D) HEK293T cells were transfected with the indicated plasmids and ISRE-Luc reporter. Cell lysates were analyzed by luciferase (top) and immunoblotting (bottom) assays.
(E) HEK293T cells stably expressing FLAG-STING were transfected with increasing doses of Myc-Ku80 or empty vector. At 24 h after transfection, the cells were stimulated with cGAMP (25 ng/mL) for 4 h and analyzed by qPCR (top) and immunoblotting (bottom).
(F) THP-1 cells stably expressing shRNA targeting Ku80 or control cells were stimulated with cGAMP (1 ng/mL) for 4 h or HT-DNA (1 μ g/mL) for 6 h, or infected with HSV-1 (10 MOI) for 9 h, and then analyzed by qPCR to quantify *IFNB1* mRNA.
(G) Similar to (F), except the cells were treated with ISD, HT-DNA, and cGAMP, followed by immunoblotting analysis.
(H) Wild-type and cGAS knockout THP-1 cells were infected with shRNA lentivirus targeting Ku80 or control empty vector for 48 h and then infected with HSV-1 (10 MOI) for 9 h. *IFNB1* mRNA was quantified by qPCR.
(I) HEK293T cells were co-transfected with the indicated plasmids and then analyzed by colP with anti-FLAG M2 agarose beads and immunoblotting.
Data shown in (A–F and H) are from one representative experiment of at least three independent experiments (mean \pm SD, n = 3 biological replicates in [A–D] and technical replicates in [E, F, and H]). *p < 0.05, **p < 0.01, ***p < 0.001; n.s., not significant; two-tailed Student's t test. See also Figure S5.

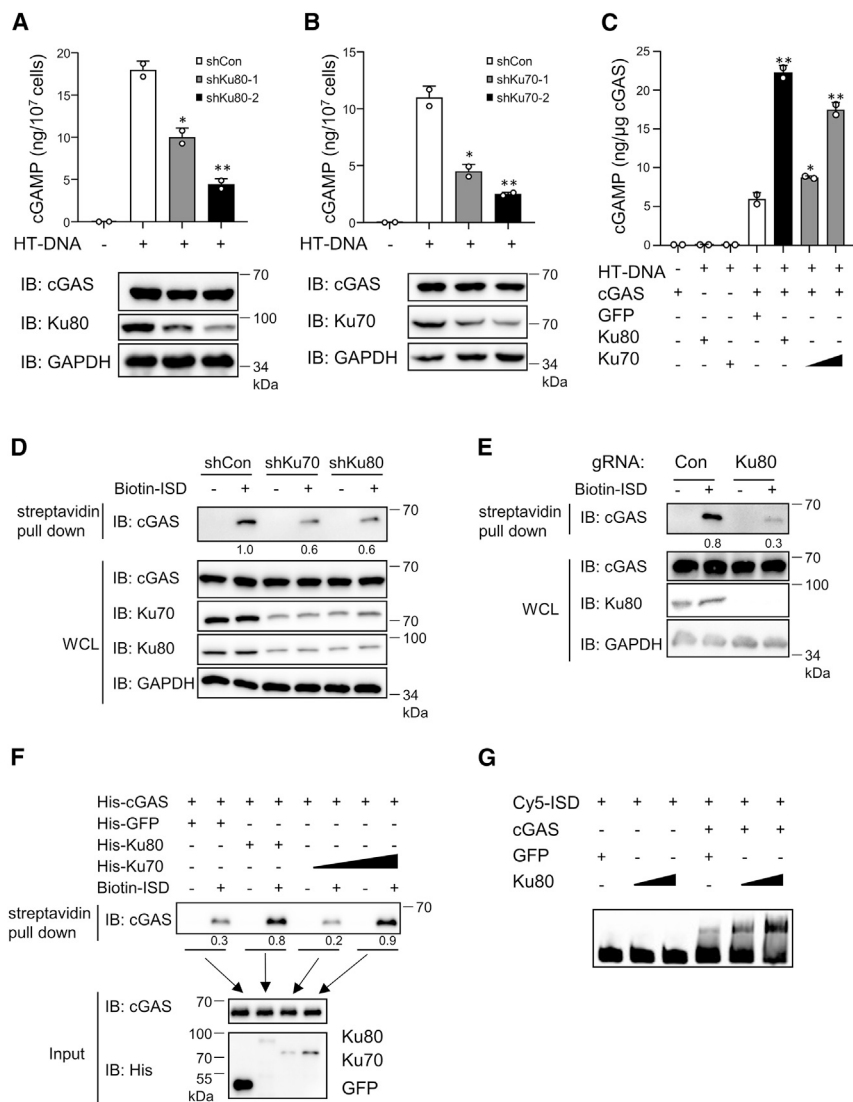


Figure 4. Ku proteins augment cGAS catalytic activity by promoting cGAS-DNA binding

(A and B) Ku80- (A) or Ku70- (B) knockdown and control THP-1 cells were stimulated with HT-DNA (1 μg/mL) for 6 h. The cells were harvested for cGAMP measurement by ELISA (top) and immunoblotting assay (bottom).

(C) Recombinant cGAS (0.5 μM) and GFP (4 μM), Ku80 (0.9 μM), or Ku70 (0.9 or 4 μM) were incubated with HT-DNA (0.2 μg/μL). cGAMP production was measured by ELISA.

(D) Ku80- or Ku70-knockdown and control THP-1 cells were transfected with biotin-ISD (1 μg/mL) for 2 h. The cell lysates were incubated with streptavidin-Sepharose beads for 4 h and analyzed by immunoprecipitation and immunoblotting.

(E) Similar to (D), except wild-type and Ku80-deficient HeLa cells were used.

(F) Recombinant cGAS protein (3.4 nM) together with GFP (100 nM), Ku80 (5 nM), or Ku70 (5 or 100 nM) was incubated with streptavidin-Sepharose beads with or without biotin-ISD (1 μg) for 3 h and then pulled down with streptavidin-Sepharose beads and analyzed by immunoblotting.

(G) Recombinant GFP (5.5 nM) or Ku80 (2.75 or 5.5 nM) was incubated with or without cGAS (100 nM) in the presence of Cy5-ISD (1.25 μM) and analyzed by EMSA to measure cGAS-DNA binding ability.

Data shown in (A–C) are from one representative experiment of at least three independent experiments (mean ± SD, n = 2 biological replicates). *p < 0.05, **p < 0.01, two-tailed Student's t test. See also Figure S6.

remarkably reduced the binding ability of cGAS to DNA in HeLa cells (Figure 4E). The *in vitro* biotin-ISD pull-down assays also supported the findings that Ku80 and Ku70 enhanced the binding of cGAS to ISD and that the effect of Ku80 was stronger than that of Ku70 (Figure 4F). To further confirm these results, we performed an electrophoretic mobility shift assay (EMSA) using purified recombinant cGAS, Ku80, and Ku70 from *E. coli*, and consistently found that Ku80 and Ku70 both promoted DNA binding of cGAS, but compared with Ku80, a high concentration of Ku70 was needed (Figures 4G and S6B). Together, these findings demonstrate that Ku80 plays a predominant role in efficient DNA binding and activation of cGAS.

Ku proteins promote cGAS condensation

Previous studies have shown that cGAS can form dimers and undergo aggregation after detecting cytosolic DNA (Du and Chen, 2018; Li et al., 2013a; Zhang et al., 2014). Based on our finding that Ku80 and Ku70 significantly increased DNA binding of

cGAS, we next investigated whether Ku80 and Ku70 modulated cGAS condensation. First, HEK293T cells were co-transfected with a mixture of hemagglutinin (HA)-cGAS and FLAG-cGAS together with Ku80, Ku70, or an empty vector, followed by coIP assays. As shown in Figure 5A, overexpression of Ku80 or Ku70 enhanced the self-association of cGAS, but Ku70 had a much weaker effect than Ku80. To confirm these results, we performed semi-denaturing detergent agarose gel electrophoresis (SDD-AGE) assays to detect cGAS condensation. The results showed that Ku80 overexpression dramatically promoted cGAS condensation in a dose-dependent manner, and that although Ku70 overexpression also promoted cGAS condensation, the effect was much weaker (Figure 5B). In addition, we performed immunostaining assays and found that cGAS formed fewer granules in Ku80- or Ku70-knockdown HeLa cells than it did in the control HeLa cells (Figure 5C). A similar result was found in Ku80-deficient HeLa cells (Figure 5D). Together, these results confirm that Ku proteins augment cGAS condensation.

Core domain of Ku proteins plays an important role in regulating cGAS activation

Our coIP experiments indicated that the Core domain of Ku80 and Ku70 was required for the interaction of cGAS with Ku

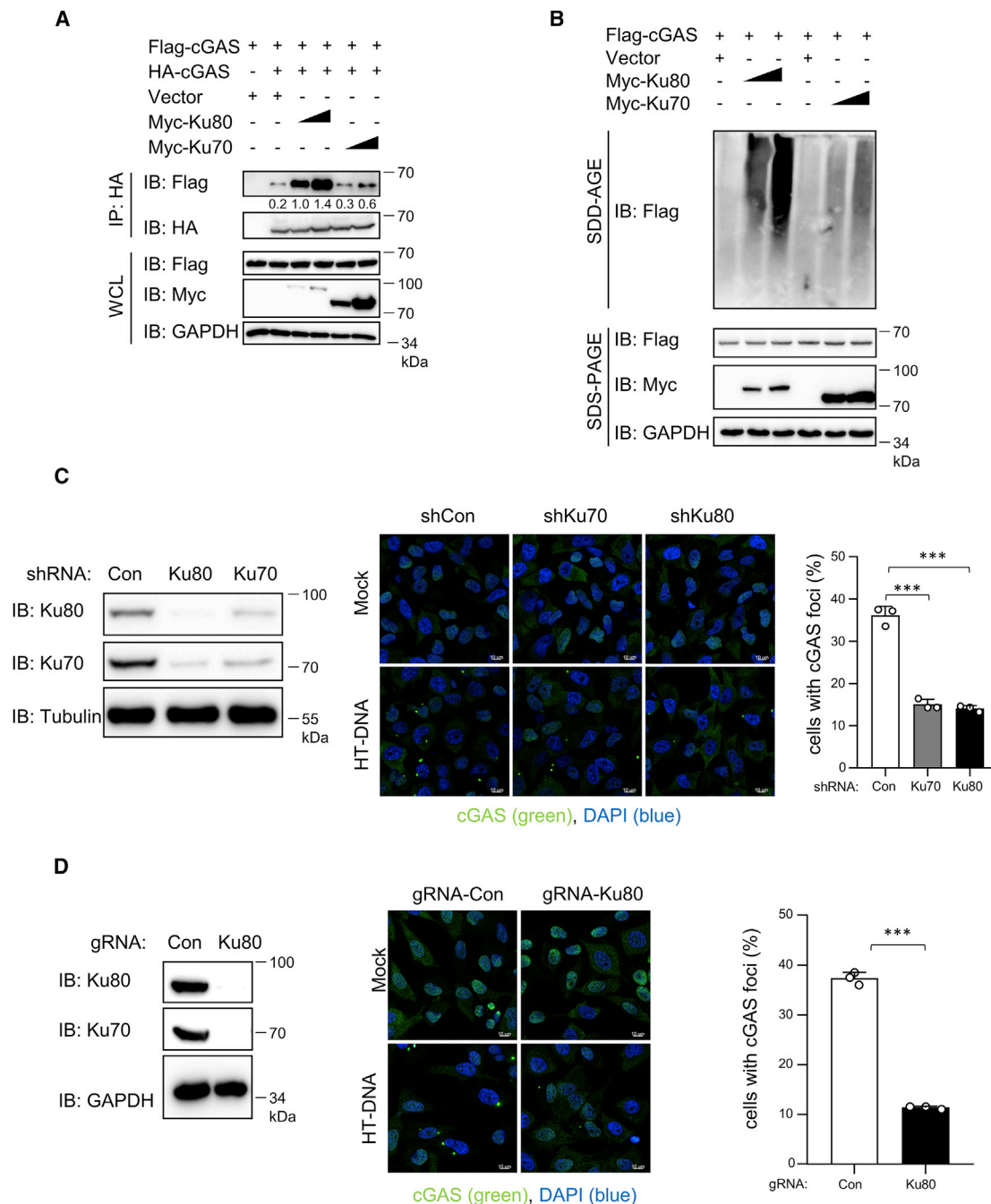


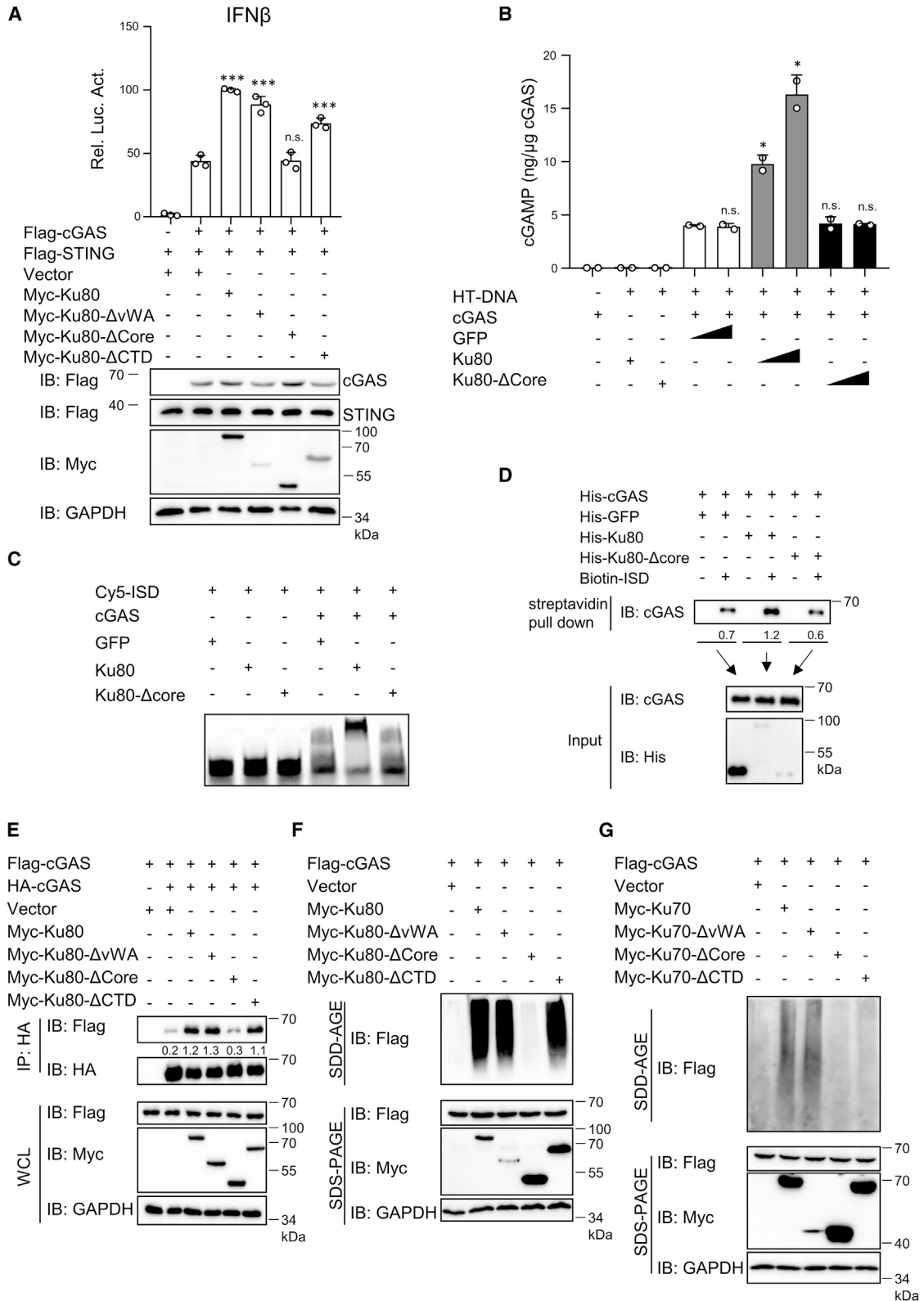
Figure 5. Ku proteins promote cGAS condensation

(A) HA-tagged cGAS and FLAG-tagged cGAS were co-transfected into HEK293T cells with increased doses of Ku80 or Ku70 expression plasmid. After 24 h of transfection, the cells were lysed for coIP and immunoblotting assays.

(B) HEK293T cells were co-transfected with the indicated plasmids. Cell lysates were resolved by SDD-AGE and SDS-PAGE and analyzed by immunoblotting.

(C) HeLa cells stably expressing shRNA targeting Ku80 or Ku70 or control empty vector (left) were treated with HT-DNA (1 μ g/mL) for 6 h, followed by immunofluorescence analysis of cGAS (green, middle). Scale bars, 10 μ m. The percentage of cells with cGAS foci was quantified, and more than 100 cells from each group were analyzed (right).

(D) Similar to (C), except wild-type and Ku80-deficient HeLa cells were used. Data shown in (C and D) are from one representative experiment of at least three independent experiments (mean \pm SD, n = 3 biological replicates). ***p < 0.001, two-tailed Student's t test.



(legend on next page)

proteins, and therefore we examined whether the Ku protein Core domain was required for the regulatory role of Ku proteins in modulating cGAS activity. First, we performed reporter assays and found that Ku80- Δ Core did not promote the activation of cGAS-STING, whereas Ku80- Δ vWA and Ku80- Δ CTD promoted the activation of cGAS-STING in a way similar to that of full-length Ku80 (Figure 6A). Second, we performed *in vitro* cGAMP synthesis assays to investigate whether the Ku80 Core domain was required for regulating cGAS activity using purified Ku80- Δ Core from *E. coli*. The results showed that, unlike wild-type Ku80, Ku80- Δ Core did not enhance cGAMP production induced by HT-DNA (Figure 6B), which suggested that the Ku80 Core domain played an important role in increasing cGAS activity by interacting with cGAS. Third, we performed EMSA to investigate the role of the Ku80 Core domain in regulating cGAS-DNA binding. As shown in Figure 6C, unlike wild-type Ku80, Ku80- Δ Core did not enhance cGAS-DNA binding. Fourth, we performed *in vitro* biotin-ISD pull-down assay, and obtained consistent results (Figure 6D). Fifth, we compared the effects of wild-type Ku80 and its deletion variants on cGAS self-association and found that, unlike wild-type Ku80, Ku80- Δ vWA, and Ku80- Δ CTD, the Ku80- Δ Core variant did not increase cGAS self-association (Figure 6E). In addition, the SDD-AGE results showed that Ku80- Δ Core did not enhance cGAS condensation (Figure 6F). Similarly, we found that, unlike wild-type Ku70, the Ku70- Δ Core variant did not increase cGAS condensation (Figure 6G). Ku70- Δ CTD also did not enhance cGAS condensation (Figure 6G), which was consistent with the coIP results that showed that the Ku70 Core domain and CTD were involved in regulating the cGAS-Ku70 interaction. Together, these results support the conclusion that the Ku Core domain plays a critical role in mediating the interaction of the Ku protein with cGAS and in augmenting cGAS-DNA binding, resulting in enhanced cGAS condensation and activity.

Ku proteins have DNA-PKcs-independent roles in regulating cGAS-STING signaling

DNA-PKcs has been shown to play an important role in regulating antiviral immune defense against DNA virus infection; however, its function remains controversial (Ferguson et al., 2012; Sun et al., 2020). To determine the precise role of DNA-PKcs in anti-DNA viral signaling, we knocked down DNA-PKcs in THP-1 cells and found that its knockdown significantly decreased the mRNA levels of *IFNB1*, *ISG56*, and *CXCL10* stimulated by HSV-1 infection and ISD transfection (Figures S7A–S7D). To confirm the knockdown results, we generated DNA-PKcs-knockout THP-1

cells and found that the mRNA levels of *IFNB1*, *ISG56*, and *CXCL10* were significantly reduced in the DNA-PKcs-knockout cells compared with their levels in control cells following stimulation with ISD transfection (Figures 7A–7C). These data suggest that DNA-PKcs positively regulates the innate immune response against DNA virus infection.

DNA-PKcs forms a heterotrimer with Ku proteins and regulates DNA double-strand break repair and V(D)J recombination (Chaplin et al., 2021; Singleton et al., 1999), and therefore we investigated whether Ku80 and Ku70 regulation of cGAS-STING signaling was dependent on DNA-PKcs. First, we knocked down Ku80 in DNA-PKcs-knockout THP-1 cells and then we stimulated with ISD. The results showed that knockdown of Ku80 in DNA-PKcs-knockout cells still reduced the mRNA levels of *IFNB1* induced by ISD (Figures 7D–7F). Consistently, we found that knockdown of Ku80 or Ku70 still attenuated cGAMP production induced by HSV-1 infection in DNA-PKcs-knockout THP-1 cells (Figure S7E). Next, DNA-PKcs-knockout HEK293T cells were co-transfected with cGAS, STING, and Ku70, Ku80, or empty vector, followed by reporter assays. The results in Figure 7G show that in the absence of DNA-PKcs, overexpression of Ku80 or Ku70 still enhanced cGAS activity. The SDD-AGE assays also showed that DNA-PKcs knockout had no obvious effect on the increased cGAS condensation induced by overexpression of Ku70 or Ku80 (Figure 7H). Combined with the coIP results, which showed that depleting DNA-PKcs had no effect on the association of cGAS with Ku proteins, these results suggest that the Ku proteins have a DNA-PKcs-independent function in regulating cGAS-STING signaling.

DISCUSSION

Innate immune responses to virus infection are triggered by the recognition of viral nucleic acids by pattern recognition receptors (Akira et al., 2006; Brubaker et al., 2015; Medzhitov, 2007). For DNA viruses, the pattern recognition receptors contain TLR9 in the endosome (Lund et al., 2003) and a variety of cytosolic receptors, such as DAI, AIM2, IFI16, DDX41, DNA-PK, MRE11, STING, SOX2, PQBP1, and cGAS (Burdette et al., 2011; Ferguson et al., 2012; Gray et al., 2016; Kondo et al., 2013; Sun et al., 2013; Takaoka et al., 2007; Unterholzner et al., 2010; Xia et al., 2015; Yoh et al., 2015; Zhang et al., 2011b). Among these, cGAS was identified as a major cytosolic sensor that detects foreign DNA from invading microbes or self-DNA and has been shown to play a critical role in innate immune responses to virus

Figure 6. Core domain of Ku proteins plays an important role in regulating cGAS activation

(A) HEK293T cells stably expressing FLAG-STING were co-transfected with the indicated plasmids, as well as IFN β -Luc and *Renilla* reporter plasmids. Cell lysates were analyzed by luciferase (top) and immunoblotting (bottom) assays.
(B) Recombinant cGAS (0.5 μ M) and GFP (0.45 or 0.9 μ M), Ku80 (0.45 or 0.9 μ M), or Ku80- Δ Core (0.45 or 0.9 μ M) were incubated with HT-DNA (0.2 μ g/ μ L). cGAMP production was measured by ELISA.
(C) Recombinant GFP (5.5 nM), Ku80 (5.5 nM), or Ku80- Δ Core (5.5 nM) was incubated with or without cGAS (100 nM) in the presence of Cy5-ISD (1.25 μ M). The reaction mixtures were analyzed by EMSA to measure cGAS-DNA binding ability.
(D) Recombinant cGAS protein (3.4 nM) together with GFP (5 nM), Ku80 (5 nM), or Ku80- Δ Core (5 nM) was incubated with streptavidin-Sepharose beads with or without biotin-ISD (1 μ g) for 3 h and subjected to immunoprecipitation and immunoblotting analysis.
(E) HEK293T cells were co-transfected with the indicated plasmids and lysed for immunoprecipitation and immunoblotting analysis.
(F and G) HEK293T cells were transfected with the indicated plasmids. Cell lysates were resolved by SDD-AGE and SDS-PAGE and analyzed by immunoblotting. Data shown in (A and B) are from one representative experiment of at least three independent experiments (mean \pm SD, n = 3 biological replicates in [A] and n = 2 biological replicates in [B]). *p < 0.05, ***p < 0.001; n.s., not significant; two-tailed Student's t test.

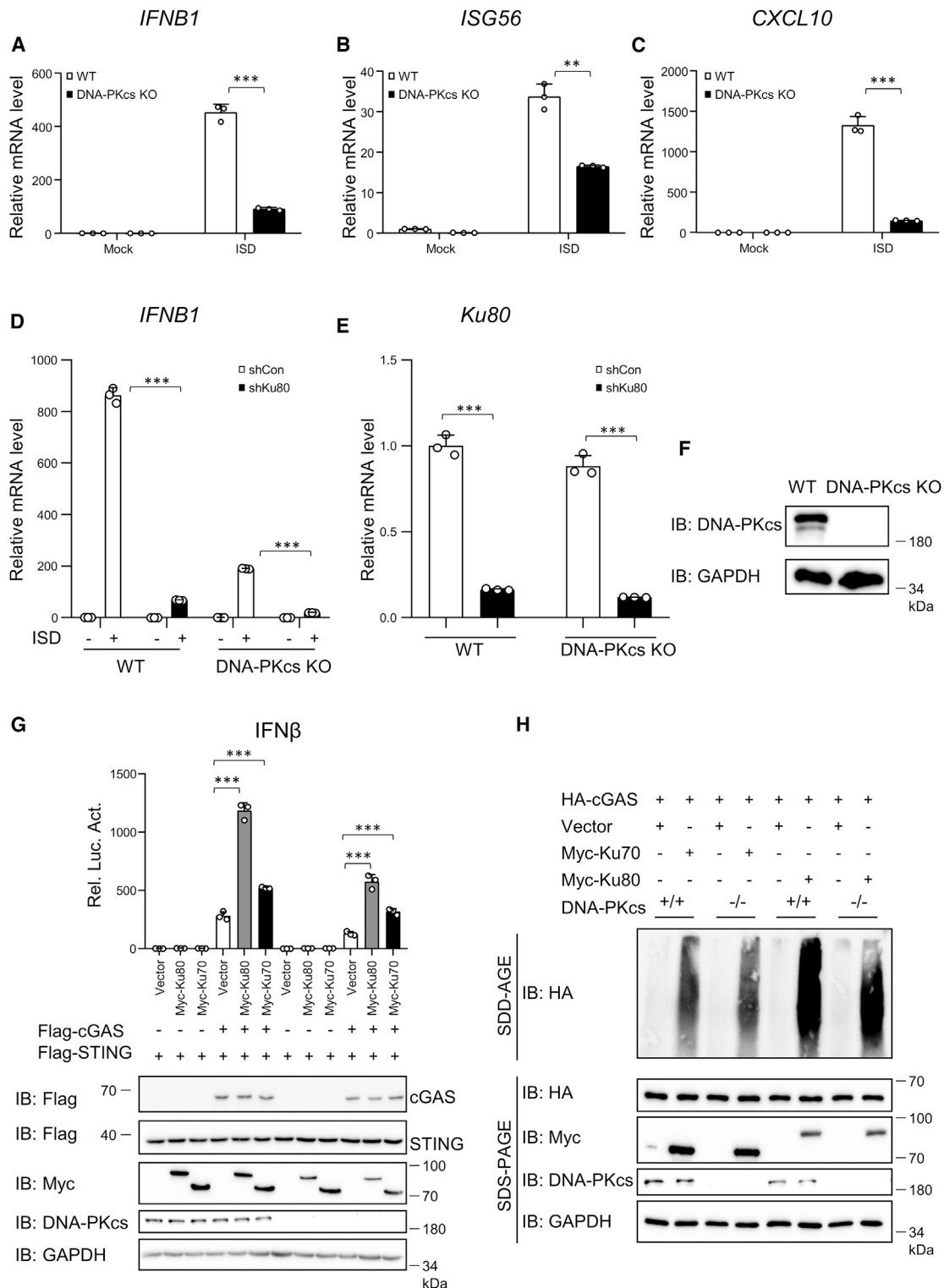


Figure 7. Ku proteins have DNA-PKcs-independent roles in regulating cGAS-STING signaling

(A–C) Wild-type (WT) and DNA-PKcs-knockout THP-1 cells were treated with ISD (2 μ g/mL) for 6 h, followed by qPCR to quantify the mRNA levels of *IFNB1* (A), *ISG56* (B), and *CXCL10* (C).

(D–F) WT and DNA-PKcs-knockout THP-1 cells were infected with shRNA lentivirus targeting Ku80 or control empty vector for 48 h and then transfected with ISD (2 μ g/mL) for 6 h. The cells were harvested for qPCR to measure the mRNA levels of *IFNB1* (D) and *Ku80* (E) or for immunoblotting to detect DNA-PKcs abundance (F).

(legend continued on next page)

infection and autoimmunity (Collins et al., 2015; Gao et al., 2015; Li et al., 2013b; Schoggins et al., 2014; West et al., 2015). However, the regulatory mechanism of cGAS activity and the relation between cGAS and other DNA sensors were still unclear. In this study, we screened for cGAS-interacting proteins by coIP combined with mass spectrometry assays and found that Ku proteins associated with cGAS through their Core domain. Functional analysis indicated that Ku proteins were required for full cGAS activity. We also provided evidence that Ku70 and Ku80 both augmented cGAS-DNA binding, leading to enhanced cGAS condensation and catalytic activity and subsequently increasing the efficiency of cGAS in the innate immune response to DNA virus infection.

Previous studies showed that the DNA-PK complex was involved in regulating innate immune signaling against DNA virus infection; however, the reported function and regulatory mechanism were controversial. A previous study showed that DNA-PK functioned upstream of STING and modulated IRF-3 activation independent of kinase activity (Ferguson et al., 2012). Another study showed that DNA-PK was found to activate STING-independent DNA sensing signaling in human cells (Burleigh et al., 2020). Unlike the positive roles in antiviral signaling described above, a recent study showed that DNA-PKcs phosphorylated cGAS and suppressed cGAS-mediated antiviral innate immune responses (Sun et al., 2020). In the present study, we found that the DNA-PK complex was a positive modulator in innate immune signaling against DNA virus infection. Interestingly, we found that Ku proteins associated with cGAS even in DNA-PKcs-knockout cells, and Ku proteins directly interacted with cGAS. These findings suggested that Ku proteins probably mediated cGAS activity in a DNA-PKcs-independent manner. Furthermore, the results of several additional experiments supported this possibility. First, the qPCR results showed that knockdown of Ku80 in DNA-PKcs-knockout cells still reduced the mRNA levels of *IFNB1* induced by ISD. Second, reporter assays demonstrated that overexpression of Ku80 or Ku70 still enhanced cGAS activity in the absence of DNA-PKcs. Third, SDD-AGE assays showed that DNA-PKcs deficiency had no effect on the increased cGAS condensation induced by overexpression of Ku70 or Ku80. Together, these findings suggest that Ku proteins can mediate cGAS-STING signaling in a DNA-PKcs-independent manner. Thus, in this study, we focused mainly on the role and regulatory mechanism of the Ku proteins in cGAS-STING signaling. The results of our various experiments demonstrated that the Ku proteins targeted cGAS to mediate cGAS-STING signaling. First, the coIP results showed that the Ku proteins associated with cGAS but not with STING. Second, the reporter assays indicated that overexpression of Ku70 and Ku80 significantly increased the activity of the ISRE reporter induced by co-expression of cGAS and STING, but not by overexpression of STING alone. Third, knockdown or deficiency of

Ku80 reduced *IFNB1* production induced by HT-DNA or HSV-1 but not by cGAMP. In addition, we found that knockdown of Ku80 failed to reduce *IFNB1* production induced by HSV-1 in cGAS knockout cells. Together, these data suggest that the Ku proteins specifically target cGAS and act upstream of STING to modulate cGAS-mediated signaling.

cGAS was reported to have poor DNA binding affinity (Jonsen et al., 2017; Kranzusch et al., 2013; Li et al., 2013a; Zhang et al., 2014) and to act as a major DNA sensor to detect low amounts of foreign DNA from invading microbes or self-DNA in the cytosol leaked from nuclear or mitochondrial compartments (Collins et al., 2015; Gao et al., 2015; Li et al., 2013b; Schoggins et al., 2014; West et al., 2015). Thus, these features of cGAS raise the possibility that there may be co-sensors that act to increase the DNA binding affinity of cGAS. In previous studies, ZCCHC3 and PCBP1 were reported to serve as co-sensors by enhancing the ability of cGAS and DNA to bind (Lian et al., 2018; Liao et al., 2021). In this study, there were several lines of evidence to support that the Ku proteins increased the binding of cGAS to DNA. First, Ku80 or Ku70 knockdown remarkably decreased the binding ability of cGAS to DNA. Second, *in vitro* biotin-ISD pull-down assays showed that Ku80 and Ku70 enhanced the binding of cGAS to ISD. Third, EMSA results also showed that the Ku proteins increased the DNA binding affinity of cGAS. These data suggest that the Ku proteins function as co-sensors of cGAS to effectively detect pathogen DNA in the cytosol, resulting in cGAS condensation and subsequently increasing cGAS activity. Previous studies have indicated that the Ku proteins and cGAS play important roles in DNA repair and cancer development (Fell and Schild-Poulter, 2015; Gullo et al., 2006; Liu et al., 2018); however, whether cGAS is regulated by the Ku proteins in these two processes needs further investigation.

In summary, we identified Ku proteins as positive modulators of the cGAS-mediated signaling pathway. The Ku proteins interacted with cGAS and promoted the DNA binding affinity of cGAS and then augmented its condensation, resulting in the enhancement of cGAS activity. Our data provide insights into the effective regulatory mechanism of cGAS-mediated innate immune signaling.

Limitations of the study

The current work has the following limitations: (1) we do not show the detailed molecular basis of how Ku proteins promote the cGAS binding to DNA; (2) because Ku70 and Ku80 form a heterodimer and the two proteins reciprocally depend on each other for stability, it is difficult to dissect the individual functions of Ku80 and Ku70 in regulating cGAS signaling *in vivo*; (3) in this work, there are no Ku-deficient mouse models to demonstrate that Ku proteins play a regulatory role in cGAS-STING signaling under physiological conditions. These issues require further investigation.

(G) WT and DNA-PKcs-knockout HEK293T cells were transfected with the indicated plasmids. Cell lysates were analyzed by luciferase (top) and immunoblotting (bottom) assays.

(H) WT and DNA-PKcs-knockout HEK293T cells were transfected with the indicated expression plasmids. Cell lysates were resolved by SDD-AGE and SDS-PAGE and analyzed by immunoblotting.

Data shown in (A–E and G) are from one representative experiment of at least three independent experiments (mean \pm SD, $n = 3$ technical replicates in [A–E] and biological replicates in [G]). ** $p < 0.01$, *** $p < 0.001$, two-tailed Student's t test. See also Figure S7.

STAR★METHODS

Detailed methods are provided in the online version of this paper and include the following:

- KEY RESOURCES TABLE
- RESOURCE AVAILABILITY
 - Lead contact
 - Materials availability
 - Data and code availability
- EXPERIMENTAL MODEL AND SUBJECT DETAILS
 - Cell lines
- METHOD DETAILS
 - Plasmids and transfection
 - Luciferase reporter assay
 - Purification of protein from *E. coli*
 - *In vivo* and *in vitro* Co-IP and immunoblotting analysis
 - *In vivo* and *in vitro* cGAS–DNA binding assay
 - Semi-denaturing detergent agarose gel electrophoresis (SDD-AGE)
 - Immunofluorescence assays
 - Antibodies
 - Viral plaque assay
 - Lentivirus-mediated generation of stable cell lines
 - qPCR
 - Electrophoretic mobility shift assay (EMSA)
 - *In vivo* cGAMP measurement
 - *In vitro* cGAMP synthesis assay
 - Mass spectrometry analysis
- QUANTIFICATION AND STATISTICAL ANALYSIS

SUPPLEMENTAL INFORMATION

Supplemental information can be found online at <https://doi.org/10.1016/j.celrep.2022.111310>.

ACKNOWLEDGMENTS

We would like to thank Dr. Daxing Gao (University of Science and Technology of China) for kindly providing HSV-1 and HSV-1-GFP viruses. This work is supported by the National Natural Science Foundation of China (grant 31970895 to Q.S.), the Basic Science Center Program of the NSFC (grant 31988101 to D.C.), and the Open Research Program of the State Key Laboratory of Membrane Biology.

AUTHOR CONTRIBUTIONS

Conceptualization, Q.S., X.T., and D.C.; methodology, Q.S., X.T., and D.C.; investigation, X.T., J.S., Y.S., Y.Z., J.Y., P.Z., and D.Z.; writing – original draft, Q.S., X.T., and D.C.; writing – review & editing, Q.S., X.T., and D.C.; funding acquisition, Q.S. and D.C. All authors provided intellectual input and vetted and approved the final manuscript.

DECLARATION OF INTERESTS

The authors declare no competing interests.

Received: March 12, 2022

Revised: June 30, 2022

Accepted: August 12, 2022

Published: September 6, 2022

REFERENCES

- Akira, S., Uematsu, S., and Takeuchi, O. (2006). Pathogen recognition and innate immunity. *Cell* 124, 783–801.
- Blier, P.R., Griffith, A.J., Craft, J., and Hardin, J.A. (1993). Binding of Ku protein to DNA. Measurement of affinity for ends and demonstration of binding to nicks. *J. Biol. Chem.* 268, 7594–7601.
- Brubaker, S.W., Bonham, K.S., Zanoni, I., and Kagan, J.C. (2015). Innate immune pattern recognition: a cell biological perspective. *Annu. Rev. Immunol.* 33, 257–290.
- Burdette, D.L., Monroe, K.M., Sotelo-Troha, K., Iwig, J.S., Eckert, B., Hyodo, M., Hayakawa, Y., and Vance, R.E. (2011). STING is a direct innate immune sensor of cyclic di-GMP. *Nature* 478, 515–518.
- Burleigh, K., Maltbaek, J.H., Cambier, S., Green, R., Gale, M., Jr., James, R.C., and Stetson, D.B. (2020). Human DNA-PK activates a STING-independent DNA sensing pathway. *Sci. Immunol.* 5, eaba4219.
- Chaplin, A.K., Hardwick, S.W., Liang, S., Kefala Stavridi, A., Hnizda, A., Cooper, L.R., De Oliveira, T.M., Chirgadze, D.Y., and Blundell, T.L. (2021). Dimers of DNA-PK create a stage for DNA double-strand break repair. *Nat. Struct. Mol. Biol.* 28, 13–19.
- Civril, F., Deimling, T., de Oliveira Mann, C.C., Ablasser, A., Moldt, M., Witte, G., Hornung, V., and Hopfner, K.P. (2013). Structural mechanism of cytosolic DNA sensing by cGAS. *Nature* 498, 332–337.
- Collins, A.C., Cai, H., Li, T., Franco, L.H., Li, X.D., Nair, V.R., Scharn, C.R., Stamm, C.E., Levine, B., Chen, Z.J., et al. (2015). Cyclic GMP-AMP synthase is an innate immune DNA sensor for *Mycobacterium tuberculosis*. *Cell Host Microbe* 17, 820–828.
- Du, M., and Chen, Z.J. (2018). DNA-induced liquid phase condensation of cGAS activates innate immune signaling. *Science* 361, 704–709.
- Fell, V.L., and Schild-Poulter, C. (2015). The Ku heterodimer: function in DNA repair and beyond. *Mutat. Res. Rev. Mutat. Res.* 763, 15–29.
- Ferguson, B.J., Mansur, D.S., Peters, N.E., Ren, H., and Smith, G.L. (2012). DNA-PK is a DNA sensor for IRF-3-dependent innate immunity. *Elife* 1, e00047.
- Gao, D., Li, T., Li, X.D., Chen, X., Li, Q.Z., Wight-Carter, M., and Chen, Z.J. (2015). Activation of cyclic GMP-AMP synthase by self-DNA causes autoimmune diseases. *Proc. Natl. Acad. Sci. USA* 112, E5699–E5705.
- Gao, P., Ascano, M., Wu, Y., Barchet, W., Gaffney, B.L., Zillinger, T., Serganov, A.A., Liu, Y., Jones, R.A., Hartmann, G., et al. (2013a). Cyclic [G(2', 5')pA(3', 5')p] is the metazoan second messenger produced by DNA-activated cyclic GMP-AMP synthase. *Cell* 153, 1094–1107.
- Gao, P., Ascano, M., Zillinger, T., Wang, W., Dai, P., Serganov, A.A., Gaffney, B.L., Shuman, S., Jones, R.A., Deng, L., et al. (2013b). Structure-function analysis of STING activation by c[G(2', 5')pA(3', 5')p] and targeting by antiviral DMXAA. *Cell* 154, 748–762.
- Gray, E.E., Winship, D., Snyder, J.M., Child, S.J., Geballe, A.P., and Stetson, D.B. (2016). The AIM2-like receptors are dispensable for the interferon response to intracellular DNA. *Immunity* 45, 255–266.
- Gu, Y., Jin, S., Gao, Y., Weaver, D.T., and Alt, F.W. (1997). Ku70-deficient embryonic stem cells have increased ionizing radiosensitivity, defective DNA end-binding activity, and inability to support V(D)J recombination. *Proc. Natl. Acad. Sci. USA* 94, 8076–8081.
- Gullo, C., Au, M., Feng, G., and Teoh, G. (2006). The biology of Ku and its potential oncogenic role in cancer. *Biochim. Biophys. Acta* 1765, 223–234.
- Hammarsten, O., and Chu, G. (1998). DNA-dependent protein kinase: DNA binding and activation in the absence of Ku. *Proc. Natl. Acad. Sci. USA* 95, 525–530.
- Hammel, M., Yu, Y., Mahaney, B.L., Cai, B., Ye, R., Phipps, B.M., Rambo, R.P., Hura, G.L., Pelikan, M., So, S., et al. (2010). Ku and DNA-dependent protein kinase dynamic conformations and assembly regulate DNA binding and the initial non-homologous end joining complex. *J. Biol. Chem.* 285, 1414–1423.
- Huston, E., Lynch, M.J., Mohamed, A., Collins, D.M., Hill, E.V., MacLeod, R., Krause, E., Baillie, G.S., and Houslay, M.D. (2008). EPAC and PKA allow

- cAMP dual control over DNA-PK nuclear translocation. *Proc. Natl. Acad. Sci. USA* **105**, 12791–12796.
- Jackson, S.P., and Jeggo, P.A. (1995). DNA double-strand break repair and V(D)J recombination: involvement of DNA-PK. *Trends Biochem. Sci.* **20**, 412–415.
- Jonsson, K.L., Laustsen, A., Krapp, C., Skipper, K.A., Thavachelvam, K., Hottler, D., Egedal, J.H., Kjolby, M., Mohammadi, P., Prabakaran, T., et al. (2017). IFI16 is required for DNA sensing in human macrophages by promoting production and function of cGAMP. *Nat. Commun.* **8**, 14391.
- Kondo, T., Kobayashi, J., Saitoh, T., Maruyama, K., Ishii, K.J., Barber, G.N., Komatsu, K., Akira, S., and Kawai, T. (2013). DNA damage sensor MRE11 recognizes cytosolic double-stranded DNA and induces type I interferon by regulating STING trafficking. *Proc. Natl. Acad. Sci. USA* **110**, 2969–2974.
- Kranzusch, P.J., Lee, A.S.Y., Berger, J.M., and Doudna, J.A. (2013). Structure of human cGAS reveals a conserved family of second-messenger enzymes in innate immunity. *Cell Rep.* **3**, 1362–1368.
- Li, X., Shu, C., Yi, G., Chaton, C.T., Shelton, C.L., Diao, J., Zuo, X., Kao, C.C., Herr, A.B., and Li, P. (2013a). Cyclic GMP-AMP synthase is activated by double-stranded DNA-induced oligomerization. *Immunity* **39**, 1019–1031.
- Li, X.D., Wu, J., Gao, D., Wang, H., Sun, L., and Chen, Z.J. (2013b). Pivotal roles of cGAS-cGAMP signaling in antiviral defense and immune adjuvant effects. *Science* **341**, 1390–1394.
- Lian, H., Wei, J., Zang, R., Ye, W., Yang, Q., Zhang, X.N., Chen, Y.D., Fu, Y.Z., Hu, M.M., Lei, C.Q., et al. (2018). ZCCHC3 is a co-sensor of cGAS for dsDNA recognition in innate immune response. *Nat. Commun.* **9**, 3349.
- Liao, C.Y., Lei, C.Q., and Shu, H.B. (2021). PCBP1 modulates the innate immune response by facilitating the binding of cGAS to DNA. *Cell. Mol. Immunol.* **18**, 2334–2343.
- Liu, H., Zhang, H., Wu, X., Ma, D., Wu, J., Wang, L., Jiang, Y., Fei, Y., Zhu, C., Tan, R., et al. (2018). Nuclear cGAS suppresses DNA repair and promotes tumorigenesis. *Nature* **563**, 131–136.
- Lund, J., Sato, A., Akira, S., Medzhitov, R., and Iwasaki, A. (2003). Toll-like receptor 9-mediated recognition of Herpes simplex virus-2 by plasmacytoid dendritic cells. *J. Exp. Med.* **198**, 513–520.
- Medzhitov, R. (2007). Recognition of microorganisms and activation of the immune response. *Nature* **449**, 819–826.
- Nussenzweig, A., Chen, C., da Costa Soares, V., Sanchez, M., Sokol, K., Nussenzweig, M.C., and Li, G.C. (1996). Requirement for Ku80 in growth and immunoglobulin V(D)J recombination. *Nature* **382**, 551–555.
- Schoggins, J.W., MacDuff, D.A., Imanaka, N., Gainey, M.D., Shrestha, B., Eitson, J.L., Mar, K.B., Richardson, R.B., Ratushny, A.V., Litvak, V., et al. (2014). Pan-viral specificity of IFN-induced genes reveals new roles for cGAS in innate immunity. *Nature* **505**, 691–695.
- Singleton, B.K., Torres-Arzayus, M.I., Rottinghaus, S.T., Taccioli, G.E., and Jeggo, P.A. (1999). The C terminus of Ku80 activates the DNA-dependent protein kinase catalytic subunit. *Mol. Cell Biol.* **19**, 3267–3277.
- Sun, L., Wu, J., Du, F., Chen, X., and Chen, Z.J. (2013). Cyclic GMP-AMP synthase is a cytosolic DNA sensor that activates the type I interferon pathway. *Science* **339**, 786–791.
- Sun, X., Liu, T., Zhao, J., Xia, H., Xie, J., Guo, Y., Zhong, L., Li, M., Yang, Q., Peng, C., et al. (2020). DNA-PK deficiency potentiates cGAS-mediated antiviral innate immunity. *Nat. Commun.* **11**, 6182.
- Takaoka, A., Wang, Z., Choi, M.K., Yanai, H., Negishi, H., Ban, T., Lu, Y., Miyagishi, M., Kodama, T., Honda, K., et al. (2007). DAI (DLM-1/ZBP1) is a cytosolic DNA sensor and an activator of innate immune response. *Nature* **448**, 501–505.
- Unterholzner, L., Keating, S.E., Baran, M., Horan, K.A., Jensen, S.B., Sharma, S., Sirois, C.M., Jin, T., Latz, E., Xiao, T.S., et al. (2010). IFI16 is an innate immune sensor for intracellular DNA. *Nat. Immunol.* **11**, 997–1004.
- Vizcaino, J.A., Csordas, A., del-Toro, N., Dianes, J.A., Griss, J., Lavidas, I., Mayer, G., Perez-Riverol, Y., Reisinger, F., Ternent, T., et al. (2016). 2016 update of the PRIDE database and its related tools. *Nucleic Acids Res.* **44**, D447–D456.
- Walker, J.R., Corpina, R.A., and Goldberg, J. (2001). Structure of the Ku heterodimer bound to DNA and its implications for double-strand break repair. *Nature* **412**, 607–614.
- Wang, J., Kang, L., Song, D., Liu, L., Yang, S., Ma, L., Guo, Z., Ding, H., Wang, H., and Yang, B. (2017). Ku70 senses HTLV-1 DNA and modulates HTLV-1 replication. *J. Immunol.* **199**, 2475–2482.
- West, A.P., Khoury-Hanold, W., Staron, M., Tal, M.C., Pineda, C.M., Lang, S.M., Bestwick, M., Duguay, B.A., Raimundo, N., MacDuff, D.A., et al. (2015). Mitochondrial DNA stress primes the antiviral innate immune response. *Nature* **520**, 553–557.
- Wu, J., Sun, L., Chen, X., Du, F., Shi, H., Chen, C., and Chen, Z.J. (2013). Cyclic GMP-AMP is an endogenous second messenger in innate immune signaling by cytosolic DNA. *Science* **339**, 826–830.
- Xia, P., Wang, S., Ye, B., Du, Y., Huang, G., Zhu, P., and Fan, Z. (2015). Sox2 functions as a sequence-specific DNA sensor in neutrophils to initiate innate immunity against microbial infection. *Nat. Immunol.* **16**, 366–375.
- Yaneva, M., Kowalewski, T., and Lieber, M.R. (1997). Interaction of DNA-dependent protein kinase with DNA and with Ku: biochemical and atomic-force microscopy studies. *EMBO J.* **16**, 5098–5112.
- Yoh, S.M., Schneider, M., Seifried, J., Soonthornvacharin, S., Akleh, R.E., Olivieri, K.C., De Jesus, P.D., Ruan, C., de Castro, E., Ruiz, P.A., et al. (2015). PQBP1 is a proximal sensor of the cGAS-dependent innate response to HIV-1. *Cell* **161**, 1293–1305.
- Zhang, X., Brann, T.W., Zhou, M., Yang, J., Oguariri, R.M., Lidie, K.B., Imamiuchi, H., Huang, D.W., Lempicki, R.A., Baseler, M.W., et al. (2011a). Cutting edge: Ku70 is a novel cytosolic DNA sensor that induces type III rather than type I IFN. *J. Immunol.* **186**, 4541–4545.
- Zhang, X., Wu, J., Du, F., Xu, H., Sun, L., Chen, Z., Brautigam, C.A., Zhang, X., and Chen, Z.J. (2014). The cytosolic DNA sensor cGAS forms an oligomeric complex with DNA and undergoes switch-like conformational changes in the activation loop. *Cell Rep.* **6**, 421–430.
- Zhang, Z., Yuan, B., Bao, M., Lu, N., Kim, T., and Liu, Y.J. (2011b). The helicase DDX41 senses intracellular DNA mediated by the adaptor STING in dendritic cells. *Nat. Immunol.* **12**, 959–965.

STAR★METHODS

KEY RESOURCES TABLE

REAGENT or RESOURCE	SOURCE	IDENTIFIER
Antibodies		
Rabbit monoclonal anti-p-IRF3	Cell Signaling Technology	Cat#: 4947S; RRID: AB_2920548
Rabbit monoclonal anti-IRF3	Cell Signaling Technology	Cat#: 4302S; RRID: AB_2920549
Rabbit monoclonal anti-cGAS	Cell Signaling Technology	Cat#: 15102S; RRID: AB_2920550
Rabbit monoclonal anti-cGAS	Cell Signaling Technology	Cat#: 79978S; RRID: AB_2920551
Rabbit monoclonal anti-p-STING	Cell Signaling Technology	Cat#: 19781S; RRID: AB_2920552
Rabbit monoclonal anti-STING	Cell Signaling Technology	Cat#: 50494S; RRID: AB_2920553
Rabbit polyclonal anti-Ku80	Cell Signaling Technology	Cat#: 2753S; RRID: AB_2920554
Rabbit monoclonal anti-Ku70	Cell Signaling Technology	Cat#: 4588S; RRID: AB_2920555
Rabbit polyclonal anti-Flag	Sigma-Aldrich	Cat#: F7425; RRID: AB_439687
Rabbit polyclonal anti-Myc	MBL	Cat#: 562-5; RRID: AB_591116
Rabbit polyclonal anti-HA	MBL	Cat#: 561-5; RRID: AB_591844
Mouse monoclonal anti-GAPDH	Sungene Biotechnology	Cat#: KM9002; RRID: AB_2920559
Mouse monoclonal anti- α -Tubulin	Sungene Biotechnology	Cat#: KM9007; RRID: AB_2920560
Mouse monoclonal anti-Ku80	Abcam	Cat#: ab119935; RRID: AB_10899161
Rabbit monoclonal anti-DNA-PKcs	Abcam	Cat#: ab32566; RRID: AB_731981
Rabbit polyclonal anti-His	Biodragon	Cat#: B1025; RRID: AB_2920563
Rabbit polyclonal anti-GFP	Biodragon	Cat#: B1023; RRID: AB_2920564
Bacterial and virus strains		
<i>E. coli</i> BL21 (DE3)	AlpaLife	Cat#: KTSM104L
HSV-1	Daxing Gao, University of Science and Technology of China	N/A
HSV-1-GFP	Daxing Gao, University of Science and Technology of China	N/A
SeV	This paper	N/A
Chemicals, peptides, and recombinant proteins		
polyethylenimine (PEI)	Polysciences	Cat#: 24765-2
Lipofectamine 2000 reagent	Invitrogen	Cat#: 11668-019
cGAMP	Invivogen	Cat#: TLRL-NACGA
ATP	Sigma-Aldrich	Cat#: A2383
GTP	Sigma-Aldrich	Cat#: G8877
HT-DNA	Sigma-Aldrich	Cat#: D6898

(Continued on next page)

Continued		
REAGENT or RESOURCE	SOURCE	IDENTIFIER
Benzonase	Yeasen	Cat#: 20157ES60
Normal Rabbit IgG	Sigma-Aldrich	Cat#: 12-370
Protein A/G UltraLink® Resin	Pierce	Cat#: 53133
Streptavidin-Sepharose beads	GE Healthcare	Cat#: 17-5113-01
ANTI-FLAG ® M2 Affinity Gel beads	Sigma-Aldrich	Cat#: A2220
Anti-GFP Nanobody Agarose beads	AlpaLife	Cat#: KTSM1301
Ni-Sepharose beads	GE Healthcare	Cat#: 17-5318-02
Anti-HA Magnetic beads	Pierce	Cat#: 88837
S-protein Agarose beads	Millipore	Cat#: 69704
Critical commercial assays		
2'3' cGAMP ELISA Kit	Cayman	Cat#: 501700
HiScript III First-Strand cDNA Synthesis kit	Vazyme	Cat#: R312-02
Deposited data		
Mass spectrometry data of cGAS interacting proteins	This paper	dataset identifier "PXD023597 [http://www.ebi.ac.uk/pride/archive/projects/PXD023597]".
Experimental models: Cell lines		
THP-1	ATCC	TIB-202
HEK293T	ATCC	CRL-11268
HEK293A	Hongyu Deng, Institute of Biophysics, Chinese Academy of Sciences	N/A
HeLa	ATCC	CCL-2
Vero	ATCC	CCL-81
immortalized MEF	This paper	N/A
HEK293T stably expressing Flag-STING	This paper	N/A
Ku80 deficiency THP-1	This paper	N/A
Ku70 deficiency THP-1	This paper	N/A
DNA-PKcs knockout THP-1	This paper	N/A
DNA-PKcs knockout HEK293T	This paper	N/A
cGAS knockout THP-1	This paper	N/A
STING knockout THP-1	This paper	N/A
Oligonucleotides		
ISD:sense 5'-TACAGATCTACTAGTG ATCTATGACTGATCTGTACATGATCTACA-3'	This paper	N/A
sgRNA and shRNA, see Table S2	This paper	N/A
primers for qPCR, see Table S3	This paper	N/A
Recombinant DNA		
IFNβ-Luc	Hongbing Shu, Wuhan University	N/A
ISRE-Luc	Hongbing Shu, Wuhan University	N/A
NF-κB-Luc	Zhijian Chen, University of Texas, Southwestern Medical Center at Dallas	N/A
Other recombinant DNA used in this study are listed in Table S1	This paper	N/A
Software and algorithms		
GraphPad Prism 8	GraphPad	https://www.graphpad.com/guides/prism/8/user-guide/tips_for_using_prism.htm
ImageJ	NIH	https://imagej.nih.gov/ij/download.html
NIS-Elements AR Analysis 5.20.00	NIKON	https://www.microscope.healthcare.nikon.com/products/software/nis-elements
Imaris 9.5.1	IMARIS	https://imaris.oxinst.com/

RESOURCE AVAILABILITY

Lead contact

Further information and requests for resources and reagents should be directed to and will be fulfilled by the lead contact, Qinmiao Sun (qinmiaosun@ioz.ac.cn).

Materials availability

All unique/stable reagents generated in this study are available from the [lead contact](#) without restriction.

Data and code availability

- The mass spectrometry proteomics data have been deposited to the ProteomeXchange Consortium via the PRIDE partner repository ([Vizcaino et al., 2016](#)) with the dataset identifier PRIDE database: PXD023597.
- This paper does not report original code.
- Any additional information required to reanalyze the data reported in this paper is available from the [lead contact](#) upon request.

EXPERIMENTAL MODEL AND SUBJECT DETAILS

Cell lines

HEK293T, THP-1, HeLa, and Vero cells were purchased from ATCC. HEK293A was kindly provided by Dr. Hongyu Deng (Institute of Biophysics, Chinese Academy of Sciences). Immortalized MEF cells were established by overexpression of SV40 large T antigen in primary MEF cells.

HEK293T, HEK293A, HeLa, Vero, and immortalized MEF cells were cultured in Dulbecco's modified Eagle's medium (Invitrogen) containing 10% (v/v) fetal bovine serum (Invitrogen) and 1% streptomycin and penicillin. THP-1 cells were cultured in RPMI-1640 containing 10% fetal bovine serum, 1% streptomycin and penicillin, 10mM HEPES, and 10 μ M β -mercaptoethanol. All cells were maintained at 37°C in the presence of 5% CO₂ in a humidified incubator. No methods were used for cell line authentication.

METHOD DETAILS

Plasmids and transfection

The information of all plasmids used in this study was listed in [key resources table](#) and [Table S1](#). cDNA encoding cGAS, STING, Ku80, Ku70, or GFP were amplified by PCR using corresponding primers and inserted into pCDH-Flag, pCDH-SFB, pcDNA3.0-Flag, pcDNA3.0-HA, pEF-IRES-puro-Myc, or pEF-IRES-puro-HA vector for expression in mammalian cells or pET28a-His vector for expression in bacteria. For construction of cGAS, Ku70, and Ku80 mutants, DNA fragments encoding cGAS truncation mutants, Ku80 or Ku70 deletion mutants were subcloned into vectors as indicated. For construction of pET28a-His-cGAS-GFP plasmid, DNA fragments encoding cGAS and GFP were assembled to linearized pET28a-His vector using homologous recombination.

Plasmids were transfected into HEK293T cells with polyethylenimine (PEI) (Polysciences) or Lipo2000 (Invitrogen). ISD and HT-DNA were transfected with Lipo2000.

Luciferase reporter assay

A firefly luciferase reporter plasmid encoding IFN β -Luc, NF- κ B-Luc, or ISRE-Luc and a Renilla reporter plasmid were co-transfected into HEK293T cells together with the indicated expression plasmids with PEI. An empty control plasmid was added at the same time to ensure that the same amount of total DNA was transfected. At 24 h following transfection, the cells were lysed for luciferase assays and luciferase activity normalized to Renilla activity was measured.

Purification of protein from *E. coli*

pET28a-His-GFP, pET28a-His-cGAS-GFP, pET28a-His-cGAS, pET28a-His-Ku80, pET28a-His-Ku80- Δ Core, and pET28a-His-Ku70 plasmids were transformed into *E. coli* BL21 (DE3). After overnight induction with 1 mM IPTG at 16°C, the cells were harvested and sonicated in lysis buffer (20 mM Tris-Cl pH 8.0, 500 mM NaCl, 10 mM imidazole, 0.2 mM PMSF), then centrifuged at 13,000 \times g for 30 min at 4°C. The supernatant was incubated with Ni-Sepharose beads for 3 h at 4°C. After washing with buffer (20 mM Tris-Cl pH 8.0, 500 mM NaCl, 20 mM imidazole) three times, the bound protein was eluted with elution buffer (20 mM Tris-Cl pH 8.0, 300 mM NaCl, 300 mM imidazole). The proteins were dialyzed with TBS buffer (20 mM Tris-Cl pH 7.5, 150 mM NaCl, 10% glycerol) and used for the *in vitro* assays.

In vivo and *in vitro* Co-IP and immunoblotting analysis

For the *in vivo* exogenous Co-IP assay, the transfected cells were lysed in Co-IP lysis buffer (0.5% Triton X-100, 20 mM Tris-HCl pH 7.5, 150 mM NaCl, 10% glycerol, 1 mM EDTA). Clarified cell lysates were incubated with anti-FLAG M2 agarose beads or anti-HA beads for 4 h at 4°C. The immunoprecipitated complexes were washed with lysis buffer containing 300 mM NaCl three times and

subjected to immunoblotting analysis. For the semi-endogenous Co-IP, cell lysates were incubated with anti-FLAG M2 agarose beads overnight at 4°C. The immunoprecipitated complexes were washed with lysis buffer containing 150 mM NaCl three times and subjected to immunoblotting. For the endogenous Co-IP, cell lysates were incubated with cGAS antibody or IgG overnight at 4°C, and then incubated with protein A/G beads for 2 h. The immunoprecipitated complexes were washed with lysis buffer containing 150 mM NaCl three times and subjected to immunoblotting.

For the *in vitro* Co-IP, recombinant cGAS-GFP protein or GFP protein was incubated with anti-GFP agarose beads in Co-IP lysis buffer for 2 h. Then, the beads were washed with lysis buffer containing 150 mM NaCl three times and resuspended in Co-IP lysis buffer. Recombinant Ku80 or Ku70 protein was added to the GFP-bound complexes and incubated for another 4 h. The immunoprecipitated complexes were washed with lysis buffer containing 300 mM NaCl three times and subjected to immunoblotting. The gray-scale value was determined by ImageJ.

In vivo and in vitro cGAS–DNA binding assay

For the *in vivo* cGAS–DNA binding assay, the cells were transfected with biotin-ISD (1 μg/mL). Then, 2 h after transfection, the cells were lysed with TAP buffer (50 mM Tris-HCl pH 7.5, 100 mM NaCl, 5% glycerol, 0.2% NP-40, 1.5 mM MgCl₂) for 30 min, and centrifuged at 13,000 × g for 15 min at 4°C. The supernatants were incubated with Streptavidin-Sepharose beads for 4 h and washed with TAP buffer three times and subjected to immunoblotting.

For the *in vitro* cGAS–DNA binding assay, biotin-ISD was incubated with Streptavidin-Sepharose beads for 2 h, washed with TAP buffer three times, and resuspended in TAP buffer. Recombinant cGAS together with Ku80, Ku80-ΔCore, or Ku70 were added to ISD-bound complexes and incubated for another 3 h, washed with TAP buffer three times, and subjected to immunoblotting.

Semi-denaturing detergent agarose gel electrophoresis (SDD-AGE)

HEK293T cells were transfected with the indicated expression plasmids. After 24 h, the cells were lysed in buffer (0.5% Triton X-100, 20 mM Tris-HCl pH 7.5, 150 mM NaCl, 10% glycerol, 1 mM EDTA) for 30 min, and then centrifuged at 13,000 × g for 15 min at 4°C. The supernatants were mixed in 1 × SDD loading buffer (0.5 × TBE, 10% glycerol, 2% SDS, 0.0025% bromophenol blue) and loaded onto a vertical 2% agarose gel (1 × TBE, 2% agarose). Electrophoresis was performed in the 1 × TBE running buffer (1 × TBE, 0.1% SDS) for 35 min at 4°C with a constant voltage of 100 V and analyzed by immunoblotting.

Immunofluorescence assays

HeLa cells were seeded on gelatin-coated glass coverslips in 12-well plates and transfected with HT-DNA (2 μg/mL). The cells were washed with phosphate-buffered saline, fixed with 4% paraformaldehyde for 15 min, permeabilized with 0.2% Triton X-100 for 10 min, and blocked with 5% (w/v) bovine serum albumin for 30 min. Then, the cells were incubated with primary and secondary antibodies. Imaging was captured using an Andor Dragonfly 505 laser scanning system and images were analyzed by Imaris 9.5.1. For quantitative co-localization analysis, images were acquired with a Nikon A1 confocal microscope. Pearson's correlation coefficient was measured using NIS-Elements AR analysis 5.20.00 software.

Antibodies

The information of antibodies used in this study was listed in [key resources table](#). All antibodies were applicable for immunoblotting. Rabbit monoclonal anti-cGAS (Cat#: 79978S) and mouse monoclonal anti-Ku80 (Cat#: ab119935) were used in immunofluorescence. Rabbit monoclonal anti-cGAS (Cat#: 15102S) was used in immunoprecipitation.

Viral plaque assay

Wild-type and Ku80-deficient THP-1 cells were infected with HSV-1-GFP at a multiplicity of infection of 5 for 24 h, and the culture supernatants were collected and diluted to infect Vero cells. After 72 h, the Vero cells were fixed with methanol for 30 min and stained with 1% crystal violet. Plaques were counted to quantitate the viral titers as plaque-forming units per mL (p.f.u./mL).

Lentivirus-mediated generation of stable cell lines

To establish HEK293T cells with stable expression of STING, HEK293T cells were infected with lentivirus particles, which were produced by co-transfection with pCDH-Flag-STING, and packaging plasmids pSPAX2 and pMD2.G, and then selected with puromycin.

To generate Ku80, Ku70, and DNA-PKcs knockdown cells, we used pLKO.1-puro-based lentivirus expressing specific short hairpin RNAs (shRNAs) against the target gene. THP-1, HeLa, or MEF cells were infected with shRNA lentivirus targeting Ku80, Ku70, or DNA-PKcs, and then selected with puromycin. The knockdown efficiency was determined by qPCR or immunoblotting. The shRNA sequences against the target gene were listed in [Table S2](#).

To generate Ku80, Ku70, DNA-PKcs, cGAS, or STING knockout cells, the corresponding single guide RNAs (sgRNAs) were inserted into LentiCRISPRv2 vector, and the cells were infected with lentivirus containing sgRNAs targeting Ku80, Ku70, DNA-PKcs, cGAS, or STING. The infected cells were selected with puromycin. The knockout cells were verified by immunoblotting. The sgRNA sequences were listed in [Table S2](#).

qPCR

Total RNA was extracted from cells using TRIzol reagent (Invitrogen) and cDNA was synthesized using a HiScript III First-Strand cDNA Synthesis kit (Vazyme). The qPCRs were conducted using SYBR Green Master Mix (Thermo Fisher) in a CFX96 Optics Module (Bio-Rad). The $2^{-\Delta\Delta C_t}$ method was used to calculate relative gene expression levels, and the relative mRNA level for each gene was normalized to the mRNA level of *GAPDH*. Data are shown as the relative abundance of the mRNA compared with that of the control groups. All samples were assayed in triplicate. The gene-specific primers used for qPCR were listed in [Table S3](#).

Electrophoretic mobility shift assay (EMSA)

Recombinant GFP, Ku80, Ku80- Δ Core, or Ku70 were incubated with or without cGAS in the presence of Cy5-ISD in EMSA buffer (20 mM HEPES pH 7.5, 50 mM KCl, 3.5 mM DTT, 0.25% Tween-20, 2% Ficoll 400) at 25°C for 30 min. The mixtures were loaded on 6% TBE gel (6% polyacrylamide, 0.5 \times TBE, 1% glycerol, 0.1% APS, 0.1% TEMED). Electrophoresis was conducted in 0.5 \times TBE running buffer with a constant voltage of 100 V for 20 min at 4°C. The gels were scanned using a Fluorescent Image Analyzer (Typhoon FLA 9000, GE Healthcare Bio-Sciences AB).

In vivo cGAMP measurement

THP-1 cells were transfected with HT-DNA (1 μ g/mL) for 6 h or infected with HSV-1 (10 MOI) for 12 h. The cells were collected and resuspended with phosphate-buffered saline, followed by sonication and centrifugation at 13,000 \times g for 15 min at 4°C. The supernatants were then incubated with benzonase (1 U/ μ L) at 37°C for 30 min and then heated at 95°C for 5 min, followed by centrifugation at 13,000 \times g for 15 min at 4°C. Then, cGAMP in the supernatant was measured using 2'3'-cGAMP ELISA kit (Cayman).

In vitro cGAMP synthesis assay

Purified recombinant human cGAS protein was incubated with purified recombinant GFP, Ku80, Ku80- Δ Core, or Ku70 in the presence or absence of HT-DNA in reaction buffer (20 mM HEPES pH 7.5, 5 mM MgCl₂, 5 mM DTT, 150 mM NaCl, 2 mM ATP, 2 mM GTP) at 37°C for 2 h. The mixtures were incubated with benzonase (1 U/ μ L) at 37°C for 30 min, and then heated at 95°C for 5 min, followed by centrifugation. The supernatants containing cGAMP were collected and measured by 2'3'-cGAMP ELISA kit (Cayman).

Mass spectrometry analysis

To identify the proteins that interact with cGAS, HEK293A cells were infected with lentivirus expressing SFB-tagged cGAS or an empty vector for 48 h. The cells were lysed with lysis buffer (20 mM Tris-HCl pH 7.5, 150 mM NaCl, 1% NP-40, 0.5% DOC, 0.1% SDS, 10% glycerol, 1 mM EDTA, 1 mM EGTA). The clarified supernatants were immunoprecipitated using S-protein beads (Millipore) for 4 h and washed with lysis buffer containing 300mM NaCl three times. Immunoprecipitates were denatured and separated by 10% SDS-PAGE. The gel was stained with Coomassie brilliant blue and the entire lane was cut into pieces of approximately 2 mm each, followed by digestion and analysis by an Orbitrap Elite mass spectrometer (Thermo Fisher Scientific). The mass spectrometry data were analyzed using Thermo Proteome Discovery (version 2.3), and tandem mass spectra were searched against the UniProt-Homo sapiens database. Ranking of the identified proteins was based on the peptide abundance ratio of sample/control and reproducibility among the MS analyses of different samples.

QUANTIFICATION AND STATISTICAL ANALYSIS

Results of all statistical analyses are shown as mean \pm SD. Significant differences between samples under different experimental conditions were performed using two-tailed Student's t-test (GraphPad Prism 8). For all tests, p values <0.05 were considered statistically significant. All experiments were repeated independently at least three times with similar results and one representative is shown.